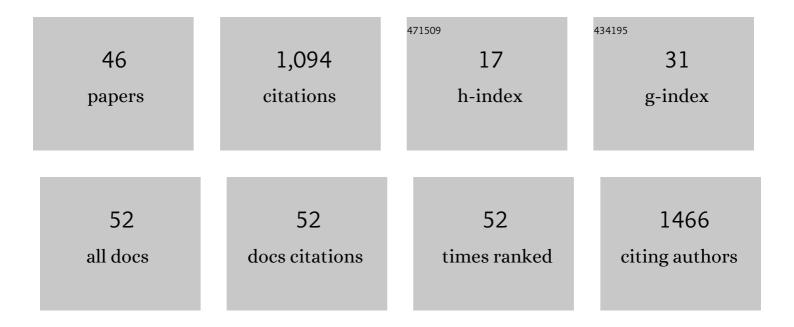
Behzad Javaheri

List of Publications by Year in descending order

Source: https://exaly.com/author-pdf/1409086/publications.pdf Version: 2024-02-01



<u> Βεμζλη Ιλυλμερι</u>

#	Article	IF	CITATIONS
1	Spatial links between subchondral bone architectural features and cartilage degeneration in osteoarthritic joints. Scientific Reports, 2022, 12, 6694.	3.3	7
2	Age and Sex Differences in Loadâ€Induced Tibial Cortical Bone Surface Strain Maps. JBMR Plus, 2021, 5, e10467.	2.7	9
3	The plate-to-rod transition in trabecular bone loss is elusive. Royal Society Open Science, 2021, 8, 201401.	2.4	3
4	A new straightforward method for semi-automated segmentation of trabecular bone from cortical bone in diverse and challenging morphologies. Royal Society Open Science, 2021, 8, 210408.	2.4	5
5	Sciatic neurectomy-related cortical bone loss exhibits delayed onset yet stabilises more rapidly than trabecular bone. Bone Reports, 2021, 15, 101116.	0.4	8
6	Characterisation of Growth Plate Dynamics in Murine Models of Osteoarthritis. Frontiers in Endocrinology, 2021, 12, 734988.	3.5	3
7	Propagation phase-contrast micro-computed tomography allows laboratory-based three-dimensional imaging of articular cartilage down to the cellular level. Osteoarthritis and Cartilage, 2020, 28, 102-111.	1.3	23
8	In situ characterization of nanoscale strains in loaded whole joints via synchrotron X-ray tomography. Nature Biomedical Engineering, 2020, 4, 343-354.	22.5	49
9	Meniscal and ligament modifications in spontaneous and post-traumatic mouse models of osteoarthritis. Arthritis Research and Therapy, 2020, 22, 171.	3.5	21
10	Loss of Adenylyl Cyclase 6 in Leptin Receptorâ€Expressing Stromal Cells Attenuates Loadingâ€Induced Endosteal Bone Formation. JBMR Plus, 2020, 4, e10408.	2.7	3
11	Applied mechanical loading to mouse hindlimb acutely increases skeletal perfusion and chronically enhanced vascular porosity. Journal of Applied Physiology, 2020, 128, 838-846.	2.5	7
12	Lasting organ-level bone mechanoadaptation is unrelated to local strain. Science Advances, 2020, 6, eaax8301.	10.3	21
13	Long-term bisphosphonate treatment coupled with ovariectomy in mice provokes deleterious effects on femoral neck fracture pattern and modifies tibial shape. Bone & Joint Open, 2020, 1, 512-519.	2.6	4
14	Conditional deletion of E11/podoplanin in bone protects against load-induced osteoarthritis. BMC Musculoskeletal Disorders, 2019, 20, 344.	1.9	13
15	Regulation of the Bone Vascular Network is Sexually Dimorphic. Journal of Bone and Mineral Research, 2019, 34, 2117-2132.	2.8	19
16	Using Cell and Organ Culture Models to Analyze Responses of Bone Cells to Mechanical Stimulation. Methods in Molecular Biology, 2019, 1914, 99-128.	0.9	0
17	Sost Haploinsufficiency Provokes Peracute Lethal Cardiac Tamponade without Rescuing the Osteopenia in a Mouse Model of Excess Glucocorticoids. American Journal of Pathology, 2019, 189, 753-761.	3.8	10
18	In Vivo Models of Mechanical Loading. Methods in Molecular Biology, 2019, 1914, 369-390.	0.9	5

Behzad Javaheri

#	Article	IF	CITATIONS
19	Aging and Mechanoadaptive Responsiveness of Bone. Current Osteoporosis Reports, 2019, 17, 560-569.	3.6	29
20	Targeted Inhibition of Aggrecanases Prevents Articular Cartilage Degradation and Augments Bone Mass in the <scp>STR</scp> /Ort Mouse Model of Spontaneous Osteoarthritis. Arthritis and Rheumatology, 2019, 71, 571-582.	5.6	10
21	Transient peak-strain matching partially recovers the age-impaired mechanoadaptive cortical bone response. Scientific Reports, 2018, 8, 6636.	3.3	21
22	Sexually dimorphic tibia shape is linked to natural osteoarthritis in STR/Ort mice. Osteoarthritis and Cartilage, 2018, 26, 807-817.	1.3	18
23	Spatial relationship between bone formation and mechanical stimulus within cortical bone: Combining 3D fluorochrome mapping and poroelastic finite element modelling. Bone Reports, 2018, 8, 72-80.	0.4	64
24	Regional diversity in the murine cortical vascular network is revealed by synchrotron X-ray tomography and is amplified with age. , 2018, 35, 281-299.		15
25	Studying Osteoarthritis Pathogenesis in Mice. Current Protocols in Mouse Biology, 2018, 8, e50.	1.2	8
26	The Mechanics of Skeletal Development. , 2018, , 25-51.		1
27	A Computed Microtomography Method for Understanding Epiphyseal Growth Plate Fusion. Frontiers in Materials, 2018, 4, 48.	2.4	13
28	The Chondro-Osseous Continuum: Is It Possible to Unlock the Potential Assigned Within?. Frontiers in Bioengineering and Biotechnology, 2018, 6, 28.	4.1	12
29	Pathogenic LRRK2 variants are gain-of-function mutations that enhance LRRK2-mediated repression of β-catenin signaling. Molecular Neurodegeneration, 2017, 12, 9.	10.8	45
30	Strain uses gap junctions to reverse stimulation of osteoblast proliferation by osteocytes. Cell Biochemistry and Function, 2017, 35, 56-65.	2.9	9
31	Hypomorphic conditional deletion of E11/Podoplanin reveals a role in osteocyte dendrite elongation. Journal of Cellular Physiology, 2017, 232, 3006-3019.	4.1	28
32	Altered Bone Mechanics, Architecture and Composition in the Skeleton of TIMP-3-Deficient Mice. Calcified Tissue International, 2017, 100, 631-640.	3.1	13
33	A distinctive patchy osteomalacia characterises <i>Phospho1</i> â€deficient mice. Journal of Anatomy, 2017, 231, 298-308.	1.5	21
34	Stable sulforaphane protects against gait anomalies and modifies bone microarchitecture in the spontaneous STR/Ort model of osteoarthritis. Bone, 2017, 103, 308-317.	2.9	19
35	Dmp1 Promoter-Driven Diphtheria Toxin Receptor Transgene Expression Directs Unforeseen Effects in Multiple Tissues. International Journal of Molecular Sciences, 2017, 18, 29.	4.1	6
36	Sost Deficiency does not Alter Bone's Lacunar or Vascular Porosity in Mice. Frontiers in Materials, 2017, 4, 27.	2.4	10

Behzad Javaheri

#	Article	IF	CITATIONS
37	Deficiency and Also Transgenic Overexpression of Timp-3 Both Lead to Compromised Bone Mass and Architecture In Vivo. PLoS ONE, 2016, 11, e0159657.	2.5	17
38	Predicting cortical bone adaptation to axial loading in the mouse tibia. Journal of the Royal Society Interface, 2015, 12, 20150590.	3.4	84
39	Phospho1 deficiency transiently modifies bone architecture yet produces consistent modification in osteocyte differentiation and vascular porosity with ageing. Bone, 2015, 81, 277-291.	2.9	36
40	In vivo mechanical loading rapidly activates β-catenin signaling in osteocytes through a prostaglandin mediated mechanism. Bone, 2015, 76, 58-66.	2.9	121
41	Excessive Growth Hormone Expression in Male GH Transgenic Mice Adversely Alters Bone Architecture and Mechanical Strength. Endocrinology, 2015, 156, 1362-1371.	2.8	23
42	Preclinical models for in vitro mechanical loading of bone-derived cells. BoneKEy Reports, 2015, 4, 728.	2.7	28
43	Deletion of a Single β-Catenin Allele in Osteocytes Abolishes the Bone Anabolic Response to Loading. Journal of Bone and Mineral Research, 2014, 29, 705-715.	2.8	104
44	Loading-related Regulation of Transcription Factor EGR2/Krox-20 in Bone Cells Is ERK1/2 Protein-mediated and Prostaglandin, Wnt Signaling Pathway-, and Insulin-like Growth Factor-I Axis-dependent. Journal of Biological Chemistry, 2012, 287, 3946-3962.	3.4	40
45	Lrp5 Is Not Required for the Proliferative Response of Osteoblasts to Strain but Regulates Proliferation and Apoptosis in a Cell Autonomous Manner. PLoS ONE, 2012, 7, e35726.	2.5	15
46	The mouse fibula as a suitable bone for the study of functional adaptation to mechanical loading. Bone, 2009, 44, 930-935.	2.9	70